Density Functional Calculations on First-Row Transition Metals

Thomas V. Russo, Richard L. Martin, and
P. Jeffrey Hay
Theoretical Division, MS B268
Los Alamos National Laboratory
Los Alamos, NM 87545
LA-UR-93-4258

February 5, 2008

Abstract

The excitation energies and ionization potentials of the atoms in the first transition series are notoriously difficult to compute accurately. Errors in calculated excitation energies can range from 1–4 eV at the Hartree-Fock level, and errors as high as 1.5eV are encountered for ionization energies. In the current work we present and discuss the results of a systematic study of the first transition series using a spin-restricted Kohn-Sham density-functional method with the gradient-corrected functionals of Becke and Lee, Yang and Parr. Ionization energies are observed to be in good agreement with experiment, with a mean absolute error of approximately 0.15eV; these results are comparable to the most accurate calculations to date, the Quadratic Configuration Interaction (QCISD(T)) calculations of Raghavachari and Trucks. Excitation energies are calculated with a mean error of approximately 0.5eV, compared with $\sim$ 1eV for the local density approximation and 0.1eV for QCISD(T). These gradient-corrected functionals appear to offer an attractive compromise between accuracy and computational effort.

1 Introduction

The accurate computation of the excitation energies and ionization potentials of the first transition metal series has proven to be a difficult problem for electronic structure theory.[1] In particular, those states which arise from configurations which involve a doubly occupied d subshell have much larger correlation energies than those which do not.[2] For example, the difference in correlation energies between the states arising from the $d^n s^2$ and d^{n+2} occupancies is of the order of 1eV for the elements Sc–V, where the high-spin d^{n+2} configuration never involves doubly occupied d orbitals, but increases to $\sim$ 4eV for the elements Mn–Ni, in which the d^{n+2} configuration has two additional filled d sublevels relative to $d^n s^2$. The root of this problem lies in the very large Coulomb interaction and consequent correlation which occurs when two electrons are required to occupy the same, relatively small, $3d$ orbital.

These errors can, in principle, be eliminated by configuration interaction (CI) calculations. Experience has shown,[3–17] however, that quite large one-electron basis sets including angular momenta at least through f functions are necessary in order to recover enough of the correlation energy to compute the energy differences reliably. Contracted basis sets of dimensions $(10s7p4d3f)$ are necessary to approach the *spdf* limit. In addition, the many-electron basis must be quite large; CI limited to single and double substitutions yields errors of the order of 0.4–0.7eV for the $d^n s^2 \rightarrow d^{n+1} s$ excitation energy for the elements to the right of the series (Mn–Cu), even when a large *spdf* basis is used and the results are corrected for relativistic contributions.

The remaining error is associated with higher order excitations, and therefore several size-extensive methods have been investigated. The most standard approach, Møller-Plesset perturbation theory, is not always adequate. In fact, for those atoms on the right hand side of the first transition series, the perturbation expansion fails dramatically and has not converged at fourth order[8,16,17] (MP4). Coupled cluster techniques, in which certain classes of excitations are summed to infinite order, give the most reliable results to date. The Quadratic Configuration Interaction (QCI) approximation investigated by Raghavachari and Trucks[16,17] reproduces the $d^n s^2 \rightarrow d^{n+1} s$ excitation energies with a mean absolute error of 0.12eV at the QCISD(T) level of theory. A similar level of accuracy is obtained for the low-lying ionization potentials.

A number of efforts have also been aimed at examining the performance of

density-functional theory (DFT).[18–22] It is somewhat difficult to make a general statement concerning the level of accuracy achieved by these methods, because the magnitude of the errors in DFT approaches depend, as expected, on the specific exchange and correlation functionals used. A good review of this area, and the general status of DFT *vs.* Hartree-Fock schemes prior to 1987 is provided by Salahub.[1] He points out that the DFT results also depend on "whether, and at what stage of the calculations spherical averaging is invoked." While most of the DFT results appear to be competitive with, or an improvement upon, Hartree-Fock theory, there are still rather large errors. Salahub concludes "the LSD [local spin density] method generally presents a reasonable semi-quantitative picture and interprets trends correctly; however, it yields quantitative errors in relative energies as large as 1 eV or so."

Nevertheless, a great deal of useful information has been obtained for inorganic complexes using the the local density approximation (LDA), i.e. the Slater exchange functional together with an electron correlation functional based on the properties of the homogeneous electron gas (e.g. the Vosko-Wilks-Nusair fit). Ziegler's recent review[23] is recommended, as are the articles in the book edited by Labanowski and Andzelm.[24] The most significant problem with this type of approach is the tendency of the LDA to overestimate molecular binding energies, sometimes by as much as 100%. A breakthrough in this regard has been the development of reliable "gradient-corrected" density functionals[25–27] (sometimes referred to as non-local functionals). In particular, the gradient-corrected exchange functional of Becke[25] leads to much improved bond energies.

Recently a number of studies of gradient-corrected DFT have begun to appear.[28–40] Geometries, vibrational frequencies, dipole moments, and other properties of small first row molecules are in reasonable agreement with experiment. A rule of thumb often mentioned is that these approaches are comparable in accuracy to MP2 theory. The gradient-corrected DFT approaches have one clear advantage, however; the heats of atomization are remarkable both for their accuracy and for the fairly modest basis sets required to achieve this accuracy. It seems apparent that the density converges much more rapidly with the one-electron basis than does the correlation energy computed from Hartree-Fock based approaches.

Given the success of gradient-corrected DFT for molecules composed of first row atoms, we were curious as to its performance for the excitation

energies and ionization potentials in the first transition series. The results of that study are reported in this paper. Section 2 reviews the methods used to study the Kohn-Sham equations, including issues regarding the basis sets, integration grids, and the details of an implementation of spin-restricted Kohn-Sham theory. The results are presented and discussed in Section 3, and the conclusions of this work reiterated in Section 4.

2 Methodology

The calculations described here were performed with the MESA suite of programs,[41] using a self-consistent Kohn-Sham (KS) procedure[42] with a finite orbital (Cartesian-Gaussian) basis expansion For the closed shell species we have implemented the Kohn-Sham equations as described by Pople, Gill and Johnson.[37] Of particular note is the fact that this formulation leads to Fock-like matrices which can be evaluated for gradient corrected functionals without evaluating the Hessian of the density. For the high-spin open-shell states we use a spin-restricted open-shell Kohn Sham (ROKS) procedure. Some form of this approach has apparently been used previously by Murray, Handy and Amos[33] to study the $^3B_1$ state of CH_2, but since they provide no details of the approach we outline our implementation briefly below. We adopt the notation of Johnson et al.[37]

2.1 ROKS formalism

One can view the Kohn-Sham equations as strictly analogous to the Hartree-Fock equations except for the replacement of the Hartree-Fock exchange operator with a local exchange-correlation potential. Given spin up and spin-down densities ρ_α and ρ_β, evaluated on a grid $\{\mathbf{r}_j\}$ in space,

$$\rho_i(\mathbf{r}_j) = \sum_{\mu\nu} P^i_{\mu\nu} \phi_\mu(\mathbf{r}_j)\phi_\nu(\mathbf{r}_j), \tag{1}$$

where $P^\alpha_{\mu\nu}$ and $P^\beta_{\mu\nu}$ are the familiar spin-up or spin-down density matrices and the ϕ's are the elements of the basis set, one can express a general functional of the density and its gradients as

$$f = f(\rho_\alpha, \rho_\beta, \gamma_{\alpha\alpha}, \gamma_{\alpha\beta}, \gamma_{\beta\beta}) \tag{2}$$

where the gradient invariants γ are defined as

$$\gamma_{\alpha\alpha} = |\nabla\rho_\alpha|^2, \gamma_{\alpha\beta} = \nabla\rho_\alpha \cdot \nabla\rho_\beta, \gamma_{\beta\beta} = |\nabla\rho_\beta|^2. \tag{3}$$

The exchange-correlation energy can be written as

$$E_{XC} = \int f(\rho_\alpha, \rho_\beta, \gamma_{\alpha\alpha}, \gamma_{\alpha\beta}, \gamma_{\beta\beta}) d\tau. \tag{4}$$

In order to solve the Kohn-Sham equations, one forms a Fock-like matrix as

$$F^i_{\mu\nu} = h_{\mu\nu} + J_{\mu\nu} + F^{XCi}_{\mu\nu} \tag{5}$$

where

$$F^{XCi}_{\mu\nu} = \int \left\{ \frac{\partial f}{\partial \rho_i}\phi_\mu\phi_\nu + \left[2\frac{\partial f}{\partial \gamma_{ii}}\nabla\rho_i + \frac{\partial f}{\partial \gamma_{ij}}\nabla\rho_j \right] \cdot \nabla(\phi_\mu\phi_\nu) \right\} d\mathbf{r}, \tag{6}$$

and $(i,j) \in \{(\alpha,\beta),(\beta,\alpha)\}$. The matrices h and J are the usual one-electron and Coulomb matrices, respectively. In spin-unrestricted Kohn-Sham (UKS) calculations, the α and β Fock matrices defined above are individually diagonalized and the solutions iterated until self-consistency is achieved. For the spin-restricted high-spin open-shell calculations, we combine these operators to obtain the analogue of a one-hamiltonian approach to Hartree-Fock theory. That is, if the orbitals are partitioned into closed, open, and virtual blocks, the matrix

$$\begin{pmatrix} F_0 & F_{CO} & F_0 \\ & F_0 & F_{OV} \\ & & F_0 \end{pmatrix} \tag{7}$$

is formed where

$$\begin{aligned} F_0 &= \frac{1}{2}(F^\alpha + F^\beta), \\ F_{CO} &= F^\beta, \\ F_{OV} &= F^\alpha. \end{aligned} \tag{8}$$

This operator is identical to Hamilton and Pulay's one-hamiltonian formulation of Hartree-Fock theory, except that the closed shell exchange matrix (K) is replaced by $F^{XC\beta}$ and the open shell exchange matrix with $F^{XC\alpha} - F^{XC\beta}$ (the unpaired electrons are assigned alpha spin). The Kohn-Sham matrix equations are solved by the usual self-consistent techniques. The open-shell DIIS scheme of Hamilton and Pulay[43] was used to accelerate convergence. The Coulomb and one-electron terms are computed analytically.

2.2 Functionals

For convenience our program calculates exchange and correlation functionals separately. For most of the present work we have used the gradient-corrected exchange functional of Becke[25] and the correlation functional of Lee, Yang and Parr.[27] We refer to this combination as B-LYP. For the copper atom we have also used Becke's functional with no correlation (B-null).

2.2.1 Becke Exchange

Becke's exchange functional, which was designed to improve upon the simple local density approximation (LDA) by yielding the correct asymptotic behavior of the exchange energy, is given by

$$f_B(\rho_\alpha, \rho_\beta, \gamma_{\alpha\alpha}, \gamma_{\beta\beta}) = \rho_\alpha^{4/3} g(x_\alpha) + \rho_\beta^{4/3} g(x_\beta) \tag{9}$$

with

$$g(x) = -\frac{3}{2}\left(\frac{3}{4\pi}\right)^{1/3} - \frac{bx^2}{1 + 6bx \sinh^{-1} x} \tag{10}$$

$$x_\alpha = \frac{\sqrt{\gamma_{\alpha\alpha}}}{\rho_\alpha^{4/3}} \tag{11}$$

$$x_\beta = \frac{\sqrt{\gamma_{\beta\beta}}}{\rho_\beta^{4/3}}. \tag{12}$$

Note that the expressions for x_α and x_β given in Reference 37 contain a typographical error. The parameter b is given by Becke,[25] $b = 0.0042$.

2.2.2 Lee-Yang-Parr correlation

The Lee-Yang-Parr (LYP) correlation functional is derived from the correlation energy formula of Colle and Salvetti,[44] derived from a consideration of short range effects in the two-particle density matrix. The functional itself, as transformed by Miehlich et al.,[45] is given by

$$f_{LYP}(\rho_\alpha, \rho_\beta, \gamma_{\alpha\alpha}, \gamma_{\alpha\beta}, \gamma_{\beta\beta}) = -\frac{4a}{1 + d\rho^{-1/3}} \frac{\rho_\alpha \rho_\beta}{\rho}$$

$$-2^{11/3}\frac{3}{10}(3\pi^2)^{2/3}ab\omega(\rho)\rho_\alpha\rho_\beta(\rho_\alpha^{8/3}+\rho_\beta^{8/3}) \quad (13)$$
$$+\frac{\partial f_{LYP}}{\partial\gamma_{\alpha\alpha}}\gamma_{\alpha\alpha}+\frac{\partial f_{LYP}}{\partial\gamma_{\alpha\beta}}\gamma_{\alpha\beta}+\frac{\partial f_{LYP}}{\partial\gamma_{\beta\beta}}\gamma_{\beta\beta}$$

with

$$\frac{\partial f_{LYP}}{\partial\gamma_{\alpha\alpha}} = -ab\omega(\rho)\left[\frac{1}{9}\rho_\alpha\rho_\beta\left\{1-3\delta(\rho)-[\delta(\rho)-11]\frac{\rho_\alpha}{\rho}\right\}-\rho_\beta^2\right], \quad (14)$$

$$\frac{\partial f_{LYP}}{\partial\gamma_{\alpha\beta}} = -ab\omega(\rho)\left\{\frac{1}{9}\rho_\alpha\rho_\beta[47-7\delta(\rho)]-\frac{4}{3}\rho^2\right\}, \quad (15)$$

$$\frac{\partial f_{LYP}}{\partial\gamma_{\beta\beta}} = -ab\omega(\rho)\left[\frac{1}{9}\rho_\alpha\rho_\beta\left\{1-3\delta(\rho)-[\delta(\rho)-11]\frac{\rho_\beta}{\rho}\right\}-\rho_\alpha^2\right], \quad (16)$$

$$\omega(\rho) = \frac{e^{-c\rho^{-1/3}}}{1+d\rho^{-1/3}}\rho^{-11/3}, \quad (17)$$

$$\delta(\rho) = c\rho^{-1/3}+\frac{d\rho^{-1/3}}{1+d\rho^{-1/3}}. \quad (18)$$

The constants a,b, c, and d used were those used by Miehlich et al.,[45] $a = 0.04918$, $b = 0.132$, $c = 0.2533$, and $d = 0.349$.

2.3 Grids and Integration Scheme

The evaluation of the exchange-correlation contribution to the Fock matrix (Eq. 6) and the total energy (Eq. 4) is done by a numerical quadrature. In this paper we report atomic results but we have implemented the more general partitioning scheme of Becke.[39] For each atom in the molecule an atomic grid is generated consisting of concentric spherical shells centered on the atom. The shells are given radii according to the Euler-MacLaurin scheme described by Murray, et al.[46]; each spherical shell has points and weights distributed on it according to the formulæ of Lebedev.[47] When the atomic grids are assembled into a molecular grid the weights are adjusted to partition the space into "fuzzy Voronoi polyhedra". For these atomic calculations the Lebedev angular grid of order 9 was used and is more than sufficient to integrate exactly all spherical harmonics which may appear in the solutions. The radial grid consisted of 100 points, and the "radial maximum" parameter chosen according to Slater's rules. In particular, we used values

of 4.59, 4.38, 4.20, 4.01, 3.82, 3.69, 3.53, 3.40, 3.27 and $3.16a_0$ for the atoms Sc–Zn, respectively. The accuracy of the radial grid was tested on copper by comparing the results using both larger (150 and 200 radial points) and smaller (50 and 75 points) grids. The use of 100 radial points yields stability in the total energy (in a.u.) to four digits past the decimal point; increasing the grid to 150 points changes only the fifth digit, and using only 50 points changes the second digit.

2.4 Basis Sets

The Kohn-Sham orbitals were expanded in a primitive Cartesian Gaussian basis set of dimension (14s9p6d). This consists of Wachters' primitive set[48] augmented with the diffuse d function recommended by Hay.[49] All six Cartesian components of the d functions were retained. Since Wachters' primitive basis was optimized for Hartree-Fock calculations, and the detailed shape of the Kohn-Sham orbitals can, in principle, be different, some attention was paid to the nature of the Kohn-Sham coefficients as an indication that the primitive basis should be modified. In general it appears that the Wachters/Hay set is adequate to expand the Kohn-Sham orbitals as well. In particular, most orbitals were described by two or more primitives with coefficients of ~ 0.5. There were a few exceptions which might warrant further study. For example, whereas the Ti $2s$ Hartree-Fock orbital involves primitives 9 and 10 with coefficients of 0.5 and 0.6, the Ti $2s$ B-LYP orbital wants to be somewhat more diffuse as reflected by coefficients for primitives 9 and 10 of 0.2 and 1.0. If one makes an even-tempered plot of the Ti s-space, it is apparent that there is a "gap", or missing s-function in the sequence which reflects the $2s/3s$ shell structure. An additional function would presumably improve the description of this core orbital and reduce the total energy somewhat, but should have little effect on the valence electron distribution or relative energy differences. Additional examples of this sort occur for atoms on the right side of the series.

We have also performed some initial investigations on contracted basis sets appropriate for use in the first transition series. These results are discussed in Section 3.3.

2.5 Convergence issues

For many of the cases described below we found that the simple ROKS procedure failed to converge. In most of these cases the cause of the failure was a tendency of the unpaired electrons to occupy different components of the $3d$ orbital from one iteration to the next. In most cases all that was required to avoid this was to employ symmetry constraints; for example, for the $3d^2 4s$ state of scandium we used the octahedral point group with inversion, and required that the two singly occupied d orbitals be those of the E_g irreducible representation, namely $d_{2z^2-x^2-y^2}$ and $d_{x^2-y^2}$. An initial guess with the proper symmetry was formed by permuting the default initial guess vectors. At each step the Fock matrix was diagonalized in the symmetrized orbital basis, and the occupied orbitals chosen so that the number of occupied orbitals in each irreducible representation remained the same as for the initial guess. Enforcing O_h symmetry also prevents the s orbitals from mixing with the d_{z^2} orbital.

While using symmetry constraints was sufficient to ensure convergence for most states, there were a few stubborn cases, such as $Sc^+(3d4s)$. In these cases there were no symmetry groups which could both prevent mixing of the s and d orbitals and still prevent unpaired d electrons from moving between degenerate symmetry-equivalent d orbitals. We resolved this problem by employing, for those cases where it was necessary, a maximum overlap condition in addition to the symmetry constraints: orbitals were filled according to the maximum overlap with the initial guess. The cases for which this was used were: $Sc^+(3d4s)$, $V(3d^4 4s)$, $Cr(3d^6)$, $Cr(3d^4 4s^2)$, $Cr^+(3d^4 4s)$, $Fe(3d^6 4s^2)$, $Fe^+(3d^6 4s)$, and $Co(3d^9)$.

3 Results

3.1 Ionization and excitation energies

The results of the B-LYP calculations of the ionization and excitation energies of the first transition series are given in Tables 1 and 2. The experimental values corrected for relativistic contributions are given in the final column of Tables 1 and 2. These values are simply the experimental results with an estimate of the differential relativistic energy subtracted out, as was done by Raghavachari and Trucks.[16,17] The estimate is based on directly computed

relativistic contributions to the Hartree-Fock energies,[2] scaled by an estimate for the effects of electron correlation. Figures 1–4 compare the B-LYP results with these corrected experimental values.

Perusal of Tables 1 and 2 shows that the B-LYP approximation gives a generally reliable picture of the relative stability of the states of the first transition series. Consider first the $d^n s^2 \rightarrow d^{n+1} s$ excitation energy shown in Figure 1. Note that the general "sawtooth" behavior in the excitation energy is faithfully reproduced by the restricted open-shell B-LYP method. Nevertheless, the ground state of the atom is predicted incorrectly in a few cases: vanadium, where B-LYP predicts the $d^4 s$ state to be more stable than $d^3 s^2$; iron, where B-LYP yields $d^7 s$ lower than $d^6 s^2$; and cobalt, where B-LYP places $d^8 s$ lower than $d^7 s^2$. A general tendency of B-LYP to favor $d^{n+1} s$ over $d^n s$ configurations is apparent in Figure 1. The $d^{n+1} s$ states are generally predicted to be too stable by ~ 0.5eV. In V, Co and Fe the experimental splitting between $d^{n+1} s$ and $d^n s^2$ states is of this order or smaller, and so the bias leads to an incorrect ordering. This tendency to favor $d^{n+1} s$ states is common to the LDA as well. Harris and Jones[18] found a bias towards $d^{n+1} s$ of ~ 1eV. Theory and experiment are compared for the $d^n s^2 \rightarrow d^{n+2}$ excitation in Figure 2. Again, the qualitative features of the trends are reproduced well, but the configurations rich in d-electrons (or poor in s-electrons) are consistently predicted to be too stable, in this case by ~ 0.8eV.

Figure 3 shows the results for the ionization potential $d^n s^2 \rightarrow d^n s$, a transition in which the number of d-electrons remains constant. Here, the B-LYP approximation is in much better agreement with experiment. This would suggest that the errors in the excitation energies of the neutral arise primarily from a tendency to overbind the d-electrons, and that the ionization potential of the s-electron is roughly correct. This conclusion is generally consistent with the results for the $d^n s^2 \rightarrow d^{n+1}$ ionization potential plotted in Figure 4. Most are underestimated consistent with a bias toward configurations rich in d-electrons, although this rule of thumb would not predict the overestimates which occur at the far right of the series.

The mean absolute errors in the B-LYP approximation for the various excitation energies are given in the final column of Table 3 , and the individual errors plotted in Figures 5 and 6. For purposes of comparison, Table 3 also contains the mean absolute errors as computed by Raghavachari and Trucks at the Hartree-Fock, Møller-Plesset, and QCISD(T) levels of approximation. For the $d^n s^2 \rightarrow d^n s$ ionization potential, the mean absolute B-LYP error

is only 0.10 eV, and compares favorably with both the MP4(0.10eV) and QCISD(T)(0.09eV) results. The B-LYP error is somewhat larger (0.21eV) for the $d^n s^2 \rightarrow d^{n+1}$ ionization, but is again competitive with the QCISD(T) approximation (0.14eV), and clearly superior to MP4. B-LYP does not perform as well for the excitation energies of the neutral, with mean absolute errors of 0.51eV and 0.76 for the $d^n s^2 \rightarrow d^{n+1} s$ and $d^n s^2 \rightarrow d^{n+2}$ transitions, respectively. The former can be compared with the QCISD(T) mean absolute error of 0.12eV. The overall mean B-LYP errors, it should be emphasized, are significantly smaller than the error from Hartree-Fock calculations, which can be as large as 4eV for the $d^n s^2 \rightarrow d^{n+2}$ excitation. QCISD(T) results were not reported for this excitation.

Thus far we have compared the gradient-corrected B-LYP DFT results with Hartree-Fock based approximations. It is also instructive to compare the B-LYP results with other gradient-corrected DFT functionals, such as the Becke-Perdew (BP) variant. Table 4 compares the mean absolute errors in B-LYP ionization potentials with the recent results of Ziegler and Li,[50] who examined both the Becke-Perdew approximation and the LDA (Slater exchange and Vosko-Wilk-Nusair correlation functionals). While it should be kept in mind that this is not a completely fair comparison of the functionals since Ziegler and Li used the spin-unrestricted version of Kohn-Sham theory and basis sets different from ours, it is interesting to note that both the B-LYP and BP functionals give quite similar results. It is also interesting that the LDA, while in worse agreement with experiment than either of the gradient-corrected approaches, performs rather well. In this series of ionization potentials, the gradient corrections do not appear to give dramatically improved results.

This observation is also in accord with the recent work of Kutzler and Painter.[51] For the s-ionization potentials, e.g., they find mean absolute errors of 0.22eV and 0.39eV for the gradient-corrected functionals of Langreth, Mehl and Hu (LMH)[52] and the generalized-gradient-approximation (GGA) of Perdew and Yue,[53] respectively. These can be compared with the B-LYP error of 0.10eV, the Becke-Perdew result of 0.16eV, and the LDA error of 0.28eV.

For the $s \rightarrow d$ excitation energies in the neutral species, the LDA meann absolute error is $\sim$ 0.85eV.[51] The B-LYP error found in the present work (0.51eV) is comparable to the GGA result ($\sim$ 0.6eV) of Kutzler and Painter, and significantly better than the LMH error ($\sim$ 1.2eV).

3.2 Analysis of B-LYP functional

Although the B-LYP error is large for the $d^n s^2 \rightarrow d^{n+1} s$ excitation energy, the fact that the qualitative features of the experimental trends are well reproduced (cf. Figure 1) suggests that this might be traced to a systematic error which could be improved with future functionals. An immediate question, then, is where does the error reside, in the exchange or correlation functional? The origin of the error is not as easy to pin down as one might think at first. Consider the $d^9 s^2 \rightarrow d^{10} s$ transition in the copper atom. The difference in the exact exchange contribution between these two states can be extracted from Hartree-Fock calculations on the two. It turns out to be -5.62eV (see Table 5). The differential exchange energy from either the B-null or B-LYP calculation is very similar (-5.69 and -5.74eV, respectively). The difference in the correlation energy between the two states can be inferred from the Hartree-Fock calculations and the experimental results; it is -1.54eV. The correlation energy from the B-LYP calculations is only -0.16eV. One thus might expect a rather large total B-LYP error of +1.26eV (-0.12eV from the exchange and +1.38eV from the correlation energy error). The actual error in the B-LYP calculation for this case is -0.2eV. The reason for this is that the B-LYP one-electron and Coulomb contributions are different from the Hartree-Fock values. The self-consistency aspect of the calculation makes a direct examination of the error difficult.

In order to make a more direct comparison, we also examined the results of the B-LYP functional being applied to the Hartree-Fock density. These numbers are also displayed in Table 5. The differential Becke exchange energy (-6.99eV) is now quite different from the B-LYP value (-5.74eV) and in significant disagreement with the Hartree-Fock value (-5.62eV). The differential LYP correlation energy is hardly changed (-0.16 and -0.18eV) and still significantly underestimated. Thus it appears that there are rather large errors in both functionals. The total B-LYP(HF) prediction is in rather good agreement with experiment, but this comes about because the overestimate of the exchange energy tends to cancel the underestimate of the correlation energy. Table 5 provides data for a similar analysis of the other states of interest in the copper atom. They are consistent with the conclusion reached above. Thus it appears that for Cu, the LYP functional underestimates the correlation energy, and that the Becke functional overestimates the exchange energies. The total exchange-correlation energy is reproduced rather

accurately, and both the B-LYP and B-LYP(HF) approaches are in good agreement with experiment.

The analysis and the discussion above leads one to conclude that the accuracy in the final B-LYP result arises from a rather fortuitous cancellation of errors in the exchange and correlation functionals. However, there appear to be some systematics to the error, as a study of Figures 5 and 6 demonstrate. With the exception of the $d^n s^2 \rightarrow d^n s$ ionization potential, in which the error is roughly linear in n, the curves typically exhibit a saw-tooth behavior, in which the error at $n = 5$(Mn) suddenly becomes more severe. At first glance, one might attempt to associate the sudden change in the error for $d^n s^2 \rightarrow d^{n+1} s$ which occurs between Cr and Mn ($n = 4$ and $n = 5$) to the sudden appearance of doubly occupied d-subshells in the $d^6 s$ state of Mn. For example, the error in the $d^4 s^2 \rightarrow d^5 s$ excitation energy is ~ -0.4eV in Cr, abruptly increasing to ~ -0.9eV for the $d^5 s^2 \rightarrow d^6 s$ excitation in Mn. Since the $d^6 s$ state is predicted to be too stable relative to $d^5 s^2$, one might conclude that the correlation functional overestimates the intra-pair d-d correlation energy. However, this argument would predict a similar increase in the error for the $d^4 s^2 \rightarrow d^6$ excitation in Cr. Figure 5 shows that this is not the case, and that the increase again occurs at Mn, this time in the $d^5 s^2 \rightarrow d^7$ excitation energy. Similarly, if one argues that the error is associated with the exchange functional and the "special" nature of the half-filled d^5 shell, then one is hard-pressed to explain why a similar jump in the error is not apparent in the $d^3 s^2 \rightarrow d^5$ excitation energy of Ti. At present we do not understand this behavior and further work is clearly warranted for this problem.

3.3 Basis Set Contractions

In order to test the functionals, we have attempted to eliminate many of the uncertainties associated with basis set incompleteness by using the fully uncontracted $(14s9p6d)$ basis of Wachters/Hay. For applications to molecules this basis is too large, and should be appropriately contracted. An obvious approach would be to use a general contraction scheme based on the Kohn-Sham orbitals obtained in this work. One might expect, however, that different contractions would be necessary for different variants of DFT; e.g., a set of contractions appropriate for LDA calculations, a different set for B-LYP, etc. For our initial investigation, we decided to test a contraction scheme

based on the Hartree-Fock orbitals. We therefore contracted the $(14s9p6d)$ primitive basis into a [6s5p3d] basis using the general contraction scheme of Raffenetti[54] and the Hartree-Fock coefficients of Wachters.[48] Specifically, the inner parts of the $1s$, $2s$, $2p$, $3s$, $3p$ and $3d$ orbitals were contracted via the HF coefficients, and the remaining, more diffuse primitives in each space were left free. These results are also presented in Tables 1 and 2. While the absolute energies were affected as expected, the excitation and ionization energies were generally changed by at most 0.02eV. The exceptions to this behavior occur for the Ni and Cu atoms, where some of the relative energies changed by as much as 0.12 eV.

4 Conclusions

We have examined the predictions of spin-restricted Kohn-Sham theory as regards the excitation and ionization energies of the members of the first transition series using the gradient-corrected density functionals of Becke and Lee, Yang and Parr.

First of all, it is important to note that the qualitative features of the trends in excitation and ionization energies (Figs. 1–4) are faithfully reproduced with a spin-restricted formulation of Kohn-Sham theory. It has sometimes been suggested in the literature that a spin-unrestricted formulation is necessary to reproduce, e.g., the break in the $d^n s^2 \rightarrow d^{n+1} s$ excitation energy which occurs at Cr (Fig. 1). This is clearly not the case. We believe this to be important, for a spin-restricted approach has the advantage that the solutions are eigenfunctions of spin and the uncontrolled spin contamination which freqently occurs in unrestricted Hartree-Fock (UHF) or Kohn-Sham (UKS) calculations on transition metal complexes is thereby avoided. We suspect that ROKS shares the disadvantages of ROHF: simple bonds will not always dissociate properly, molecules in which the qualitative electronic structure is best viewed as biradical in character may not be treated well, etc. In the present context, one might expect a significant spin polarization in the unrestricted formalism for those atomic states with a large number of unpaired d-electrons. While this can certainly lead to total energies which are significantly lower than the spin-restricted energies, it is interesting to note that the relative energies calculated by the ROKS procedure in this work are in close agreement with the UKS results of Ziegler and Li. A di-

rect comparison of ROKS *vs.* UKS is made difficult by the fact that Ziegler and Li used the Becke-Perdew functional whereas we examined Becke-LYP. The close agreement suggests, however, that neither the spin-polarization effects nor the different functionals used cause significant differences for the predictions of the ionization potentials of the first transition series.

The quantitative agreement with experiment is also encouraging. Ionization energies are observed to be in good agreement with experiment, with mean absolute errors of 0.10eV for the $d^n s^2 \rightarrow d^n s$ ionization, and a mean absolute error of 0.21eV for $d^n s^2 \rightarrow d^{n+1}$. These errors are much smaller than those obtained by Hartree-Fock, and compare favorably with the QCISD(T) results of Raghavachari and Trucks, which have mean absolute errors of 0.09 and 0.14eV, respectively. The ROKS B-LYP errors in the excitation energies are larger, 0.51eV for the $d^n s^2 \rightarrow d^{n+1} s$ excitation, as compared with an average absolute error of 0.12eV from the QCISD(T) calculations. The B-LYP approximation, like other DFT variants, consistently places the $d^{n+1} s$ states too low compared with $d^n s^2$.

A comparison of the results using the primitive (14s9p6d) basis of Wachters versus a (6s5p3d) general contraction based on Hartree-Fock coefficients shows that the contracted basis is generally in excellent agreement with the fully uncontracted basis. This demonstrates that the description of the potential in the valence region of the atom due to the core electrons is essentially the same in B-LYP and Hartree-Fock calculations. This suggests that the relativistic effective core potentials developed for the Hartree-Fock problem may be applicable to the DFT methods as well.

In summary, the spin-restricted Kohn-Sham calculations using the B-LYP functional look promising for calculations on transition metal complexes. The atomic errors are significantly smaller than the HF and MP approximations, particularly for those elements to the right of the row where the MP series is slow to converge. While not as accurate as the coupled-cluster techniques for this row, e.g. QCISD(T), B-LYP achieves a reasonable level of accuracy at a much reduced level of effort. Although it is clear that improved functionals are needed for quantitative accuracy, we expect the B-LYP functional, its variants or descendants to be increasingly used for electronic structure calculations on transition metal complexes.

5 Acknowledgments

This work was sponsored by the U.S. Department of Energy.

Atom	State	Energy (au) $(14s9p6d)$	ΔE (eV)	Energy (au) $[6s5p3d]$	ΔE (eV)	Rel. Corr. Exp.[16,17]
Sc	$3d4s^2(^2D)$	-760.6369	0.00	-760.6310	0.00	
	$3d^24s(^4F)$	-760.6132	0.64	-760.6071	0.64	1.33
	$3d^3(^4F)$	-760.5224	3.12	-760.5166	3.11	4.04
Sc^+	$3d4s(^3D)$	-760.3992	6.47	-760.3932	6.47	6.54
	$3d^2(^3F)$	-760.3925	6.65	-760.3866	6.65	6.98
Ti	$3d^24s^2(^3F)$	-849.3803	0.00	-849.3729	0.00	
	$3d^34s(^5F)$	-849.3764	0.11	-849.3691	0.10	0.69
	$3d^4(^5D)$	-849.2851	2.59	-849.2781	2.58	3.17
Ti^+	$3d^24s(^4F)$	-849.1326	6.74	-849.1252	6.74	6.80
	$3d^3(^4F)$	-849.1397	6.55	-849.1326	6.54	6.73
V	$3d^34s^2(^4F)$	-943.9282	0.00	-943.9200	0.00	
	$3d^44s(^6D)$	-943.9422	-0.38	-943.9341	-0.38	0.11
	$3d^5(^6S)$	-943.8724	1.52	-943.8646	1.50	2.24
V^+	$3d^34s(^5F)$	-943.6711	6.99	-943.6628	7.00	7.03
	$3d^4(^5D)$	-943.6913	6.45	-943.6833	6.44	6.48
Cr	$3d^44s^2(^5D)$	-1044.4196	0.00	-1044.4100	0.00	
	$3d^54s(^7S)$	-1044.4767	-1.55	-1044.4673	-1.56	-1.17
	$3d^6(^5D)$	-1044.3314	2.40	-1044.3213	2.41	3.14
Cr^+	$3d^44s(^6D)$	-1044.1533	7.25	-1044.1442	7.23	7.24
	$3d^5(^6S)$	-1044.2144	5.58	-1044.2052	5.57	5.46
Mn	$3d^54s^2(^6S)$	-1151.0244	0.00	-1151.0132	0.00	
	$3d^64s(^6D)$	-1150.9863	1.04	-1150.9747	1.05	1.97
	$3d^7(^4F)$	-1150.8728	4.13	-1150.8614	4.13	5.31
Mn^+	$3d^54s(^7S)$	-1150.7514	7.43	-1150.7401	7.43	7.38
	$3d^6(^5D)$	-1150.7126	8.48	-1150.7007	8.50	8.92
Fe	$3d^64s^2(^5D)$	-1263.7208	0.00	-1263.7145	0.00	
	$3d^74s(^5F)$	-1263.7253	-0.12	-1263.7189	-0.12	0.65
	$3d^8(^3F)$	-1263.6219	2.69	-1263.6154	2.70	3.73
Fe^+	$3d^64s(^6D)$	-1263.4303	7.90	-1263.4240	7.90	7.84
	$3d^7(^4F)$	-1263.4434	7.55	-1263.4369	7.55	7.77

Table 1: Results for B-LYP runs on the transition metals.

Atom	State	Energy (au) $(14s9p6d)$	ΔE (eV)	Energy (au) $[6s5p3d]$	ΔE (eV)	Rel. Corr. Exp.[16,17]
Co	$3d^7 4s^2(^4F)$	-1382.7912	0.00	-1382.7831	0.00	
	$3d^8 4s(^4F)$	-1382.8076	-0.45	-1382.7996	-0.45	0.17
	$3d^9(^2D)$	-1382.7139	2.10	-1382.7057	2.11	2.95
Co^+	$3d^7 4s(^5F)$	-1382.4850	8.33	-1382.4769	8.33	8.20
	$3d^8(^3F)$	-1382.5179	7.43	-1382.5098	7.43	7.40
Ni	$3d^8 4s^2(^3F)$	-1508.3439	0.00	-1508.3289	0.00	
	$3d^9 4s(^3D)$	-1508.3716	-0.75	-1508.3592	-0.82	-0.33
	$3d^{10}(^1S)$	-1508.3199	0.65	-1508.3060	0.62	1.24
Ni^+	$3d^8 4s(^4F)$	-1508.0225	8.75	-1508.0079	8.73	8.56
	$3d^9(^2D)$	-1508.0751	7.31	-1508.0612	7.28	7.08
Cu	$3d^9 4s^2(^2D)$	-1640.5003	0.00	-1640.4797	0.00	
	$3d^{10} 4s(^2S)$	-1640.5758	-2.05	-1640.5586	-2.15	-1.85
Cu^+	$3d^9 4s(^3D)$	-1640.1676	9.05	-1640.1444	9.12	8.92
	$3d^{10}(^1S)$	-1640.2753	6.12	-1640.2590	6.00	5.65
Zn	$3d^{10} 4s^2(^1S)$	-1779.4837	0.00	-1779.4656	0.00	
Zn^+	$3d^{10} 4s(^2S)$	-1779.1345	9.50	-1779.1169	9.49	9.23
	$3d^9 4s^2(^2D)$	-1778.8256	17.91	-1778.8048	17.98	17.85

Table 2: Results for B-LYP runs on the transition metals(continued).

Ionization	HF	MP2	MP3	MP4	QCISD(T)	B-LYP
$d^n s^2 \rightarrow d^n s$	1.43	0.32	0.31	0.10	0.09	0.10
$d^n s^2 \rightarrow d^{n+1}$	0.75	0.52	0.43	0.38	0.14	0.22
Excitations						
$d^n s^2 \rightarrow d^{n+1} s$	0.77	0.49	0.53	0.41	0.12	0.51
$d^n s^2 \rightarrow d^{n+2}$						0.76

Table 3: Comparison of mean absolute deviations for the ionization and excitation energies of the first row transition metals. The B-LYP results are those of the current work, all others are taken from Raghavachari and Trucks (RT).[17,16] Errors are relative to the experimental values with relativistic corrections.

Ionization	LDA[a]	B-P[b]	B-LYP[c]
$d^n s^2 \rightarrow d^n s$	0.28	0.16	0.10
$d^n s^2 \rightarrow d^{n+1}$	0.27	0.23	0.22

Table 4: Comparison of mean absolute deviations (eV) for the ionization potentials of the first row transition metals. [a] Slater Exchange with VWN correlation functional[50] [b] Becke Exchange with Perdew Correlation Functional.[50] [c] Present work.

$d^9s^2 \rightarrow d^{10}s$	HF	B-null	B-LYP	B-LYP(HF)
ΔE_{exch}	-5.62	-5.69	-5.74	-6.99
ΔE_{corr}	-1.54	0.00	-0.16	-0.18
ΔE_{coul}	185.18	153.30	154.01	185.18
Δh_1	-179.88	-149.50	-150.16	-179.88
E_{total}		-1.89	-2.05	-1.86
$d^9s^2 \rightarrow d^9s$				
ΔE_{exch}	3.40	4.18	4.23	4.12
ΔE_{corr}	1.57	0.00	0.92	0.92
ΔE_{coul}	-255.57	-259.55	-264.33	-255.57
Δh_1	259.52	263.60	268.23	259.52
E_{total}		8.23	9.05	8.98
$d^9s^2 \rightarrow d^{10}$				
ΔE_{exch}	-2.51	-1.53	-1.49	2.90
ΔE_{corr}	-0.45	0.00	0.40	0.31
ΔE_{coul}	-60.38	-95.15	-98.52	-60.38
Δh_1	69.00	102.41	105.73	69.00
E_{total}		5.73	6.12	6.02

Table 5: Breakdown of energy contributions for B-LYP, B-null, HF and B-LYP(HF) (B-LYP using Hartree-Fock density) calculations on Cu. For the HF case E_{corr} is the empirical correlation, $E_{exp} - E_{HF}$

6 Figure Captions

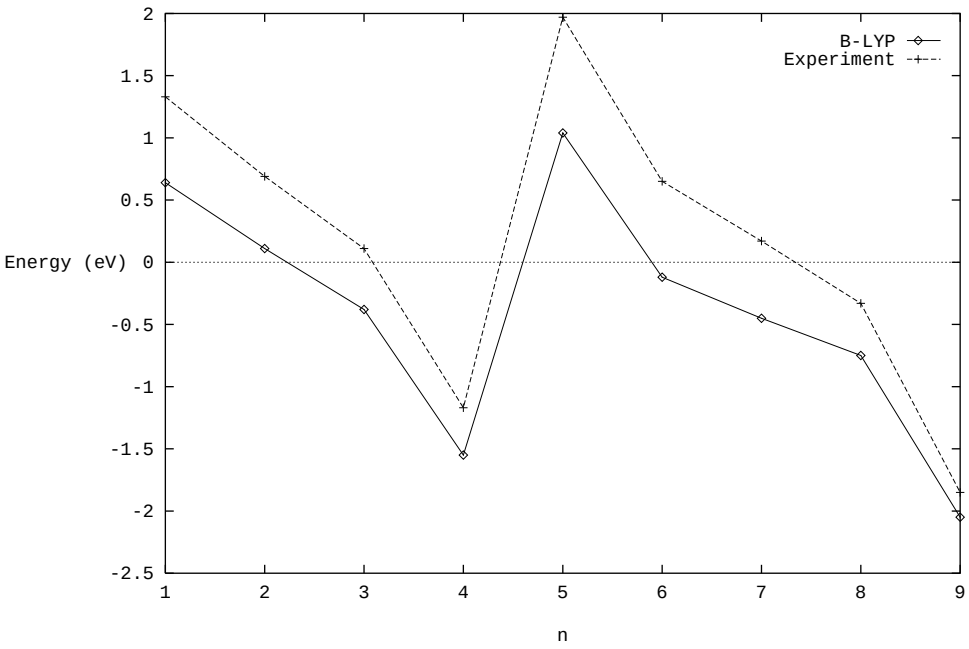

Figure 1: Plot of experimental and B-LYP values for the interconfigurational energy between the $d^n s^2$ and $d^{n+1} s$ states for the first transition series. Diamonds are B-LYP values, plusses are experimental values with relativistic corrections.

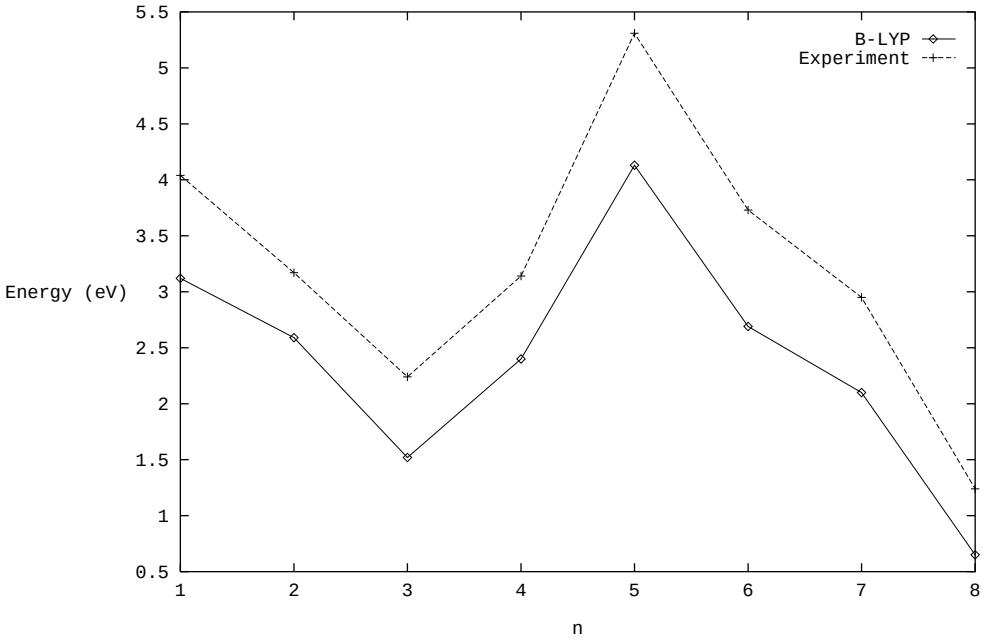

Figure 2: Plot of experimental and B-LYP values for the interconfigurational energy between the $d^n s^2$ and d^{n+2} states for the first transition series. Diamonds are B-LYP values, plusses are experimental values with relativistic corrections.

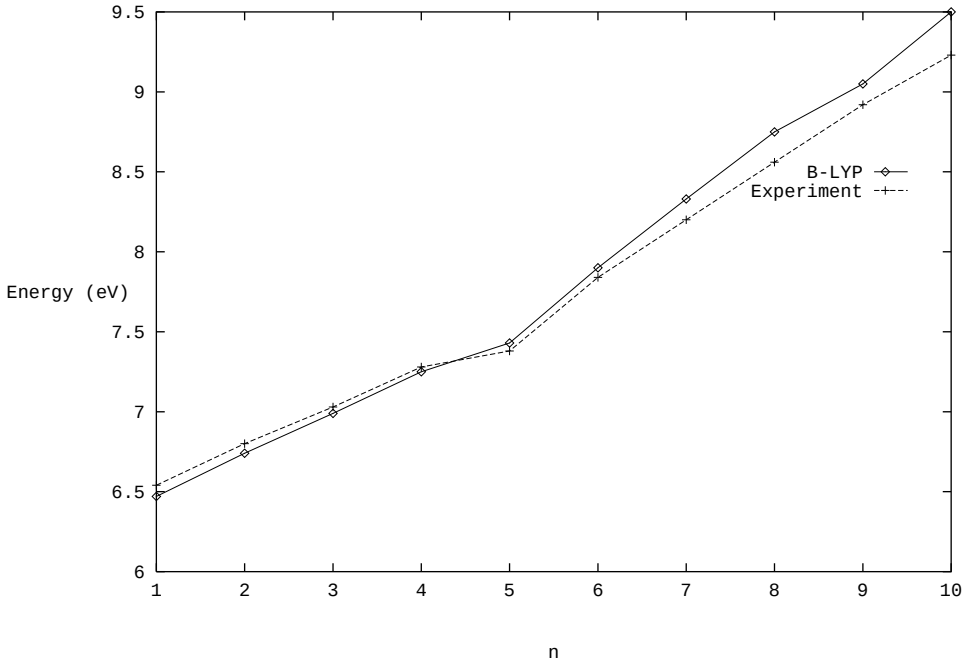

Figure 3: Plot of experimental and B-LYP values for the interconfigurational energy between the $d^n s^2$ and $d^n s$ states for the first transition series. Diamonds are B-LYP values, plusses are experimental values with relativistic corrections.

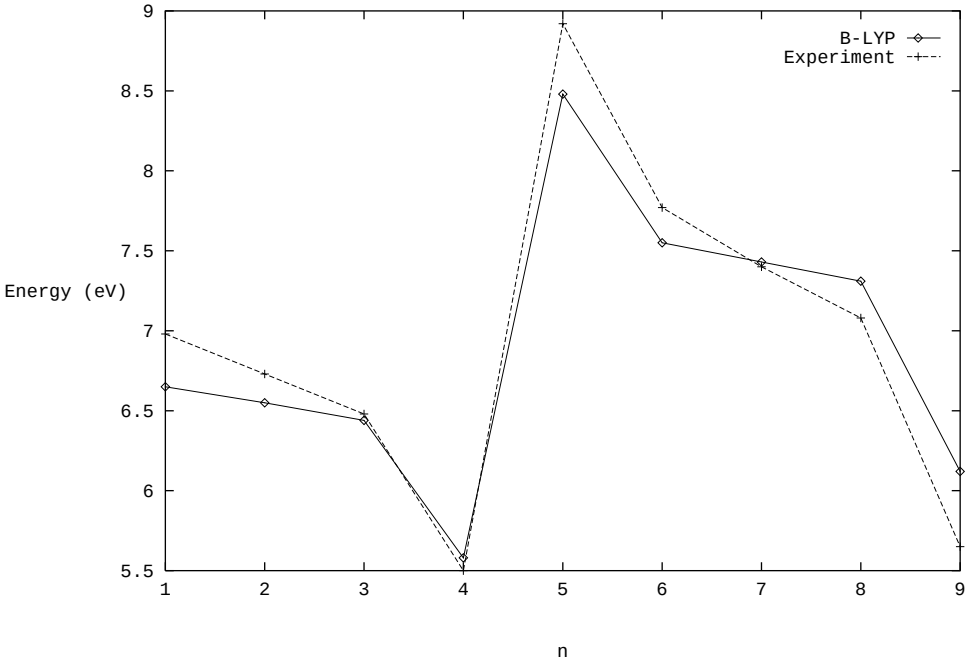

Figure 4: Plot of experimental and B-LYP values for the interconfigurational energy between the $d^n s^2$ and d^{n+1} states for the first transition series. Diamonds are B-LYP values, plusses are experimental values with relativistic corrections.

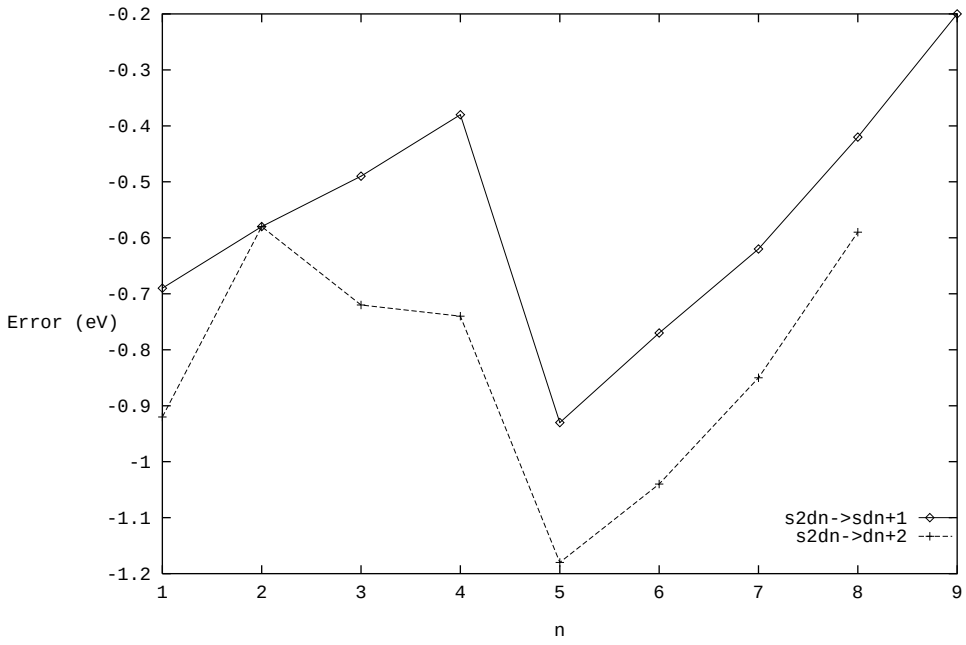

Figure 5: Plot of difference between experimental values and B-LYP values of excitation energies for the first row transition metals. Diamonds are the $s^2d^n \rightarrow sd^{n+1}$ excitation energy, plusses are $s^2d^n \rightarrow d^{n+2}$.

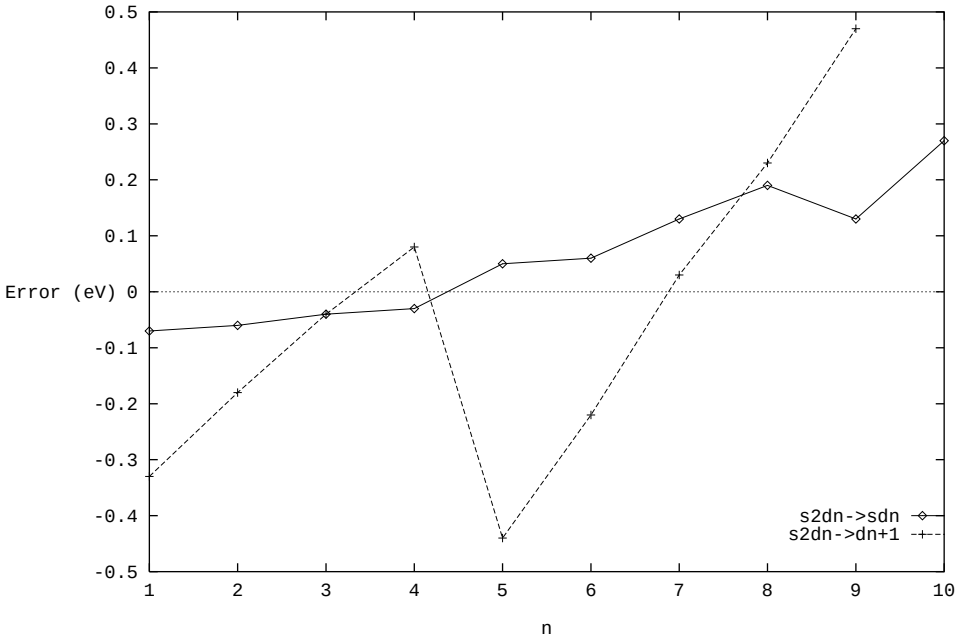

Figure 6: Plot of difference between experimental values and B-LYP values of ionization potentials for the first row transition metals. Diamonds are the $s^2d^n \rightarrow sd^n$ ionization potential, plusses are $s^2d^n \rightarrow d^{n+1}$.

References

[1]For a review of the status of this area prior to 1987, see D.R. Salahub, *Advances in Chemical Physics*, K.P. Lawley, ed., Vol. LXIX, 447 (1987)

[2]R. L. Martin and P. J. Hay, *J. Chem. Phys* **75**,4539–4545 (1981).

[3]M. Guse, N.S. Ostlund and G.D. Blyholder, *Chem. Phys. Lett.* **61**, 526–531(1979).

[4]T.H. Dunning, B.H. Botch and J.F. Harrison, *J. Chem. Phys.* **72**,3419–3420; B.H. Botch, T.H. Dunning and J.F. Harrison, *J. Chem. Phys.* **75**, 3466–3476(1981).

[5]R.L. Martin, *Chem. Phys. Lett.* **75**,290–293(1980).

[6]C.W. Bauschlicher, S.P. Walch and H. Partridge, *J. Chem. Phys.* **76**,1033–1039(1982).

[7]Y.S. Lee and K.F. Freed, *J. Chem. Phys.* **77**,1984–2001(1982); *ibid.* **79**, 839–851(1983).

[8]C.M. Rohlfing and R.L. Martin, *Chem. Phys. Lett.* **115**,104–107(1985).

[9]K.K. Sunil and K.D. Jordan, *J. Chem. Phys.* **82**,873–880(1985).

[10]K. Raghavachari, K.K. Sunil and K.D. Jordan *J. Chem. Phys.* **83**,4633–4640(1985).

[11]S.R. Langhoff and C.W. Bauschlicher, *J. Chem. Phys.* **84**,4485–4488(1986).

[12]E.A. Salter, L. Adamowicz and R.J. Bartlett, *Chem. Phys. Lett.* **122**,23–28(1985); *ibid.* **130**,152–153(1986).

[13]C.M. Rohlfing, *Chem. Phys. Lett.* **127**,183–184(1986).

[14]C.W. Bauschlicher, *J. Chem. Phys.* **86**,5591–5594(1987).

[15]C.W. Bauschlicher, P.E.M. Siegbahn and L.G.M. Pettersson, *Theor. Chim. Acta* **74**, 479(1988).

[16]K. Raghavachari and G.W. Trucks *J. Chem. Phys* **91**, 1062–1065 (1989).

[17]K. Raghavachari and G.W. Trucks *J. Chem. Phys* **91**, 2457–2460 (1989).

[18]J. Harris and R.O. Jones, *J. Chem. Phys* **79**, 1874 (1983); *J. Chem. Phys.* **68**, 3316 (1978).

[19]J.P. Perdew and A. Zunger, *Phys. Rev. B* **23**, 5048 (1981).

[20]O. Gunnarrsson and R.O. Jones, *Solid State Commun.* **37**, 249 (1981).

[21]J.G. Harrison, *J. Chem. Phys* **78**, 4562 (1983).

[22]S. Baroni, *J. Chem. Phys.* **80**, 5703 (1984).

[23]T. Ziegler, *Chem. Rev.* **91**, 651 (1991).

[24]J. Labanowski and J. Andzelm, eds., *Density Functional Methods in Chemistry*, Springer–Verlag, Heidelberg (1991).

[25]A.D. Becke, *Phys. Rev. A* **38**, 3098 (1988).

[26]J.P. Perdew, *Phys. Rev. B* **33**, 8822 (1986); *Phys. Rev. B* **34**, 7406 (1986).

[27]C. Lee, W. Yang and R.G. Parr *Phys. Rev. B* **37**,785–789(1988).

[28]A.D. Becke, *J. Chem. Phys.* **96**, 2155(1992).

[29]P.M.W. Gill, B.G. Johnson, J.A. Pople and M.J. Frisch, *Chem. Phys. Lett.* **197**,499 (1992).

[30]B.G. Johnson, P.M.W. Gill, and J.A. Pople, *J. Chem. Phys.* **97**, 7846 (1992).

[31]R.H. Dickson and A.D. Becke, *J. Chem. Phys.* **98**, 3898 (1993).

[32]T. Zhu, C. Lee and W. Yang, *J. Chem. Phys. J. Chem. Phys.* **98**, 4814(1993).

[33]C.W. Murray, N.C. Handy and R.D. Amos, *J. Chem. Phys.* **98**,7145–7151(1993).

[34]N.C. Handy, C.W. Murray and R.D. Amos, *J. Chem. Phys.* **97**, 4392 (1993).

[35]C.W. Murray, G.J. Laming, N.C. Handy and R.D. Amos, *Chem. Phys. Lett.* **199**, 551 (1992).

[36]J. Andzelm, C. Sosa and D.A. Eades, *J. Phys. Chem.* **97**, 4664 (1993).

[37]B.G. Johnson, P.M.W. Gill and J.A. Pople, *J. Phys. Chem* **98**, 5612–5626 (1993).

[38]J.A. Pople, P.M.W. Gill and B.G. Johnson, *Chem. Phys. Lett.* **199**,557–560 (1992).

[39]A.D. Becke *J. Chem. Phys* **88** (4) 2547–2553 (1988).

[40]G.E. Scuseria, *J. Chem. Phys.* **97**, 7528 (1992).

[41]MESA, B.H. Lengsfield III, R.L. Martin, P.W. Saxe, T.V. Russo, M. Page, B. Schneider, M.O. Braunstein, P.J. Hay, A.K. Rappe (1993).

[42]W. Kohn and L.J. Sham *Phys. Rev* **140**,4A, A1133–A1138 (1965).

[43]T.P. Hamilton and P. Pulay *J. Chem. Phys.* **84**,5728–5734 (1986).

[44]R. Colle and O. Salvetti, *Theoret. Chim. Acta* **37**,329 (1975).

[45]B. Miehlich, A. Savin, H. Stoll, H. Preuss *Chem. Phys. Lett.* **157**,200–206(1989).

[46]C.W. Murray, N.C. Handy, and G.J. Laming, *Mol. Phys.* **78**, 997(1993).

[47]V.I. Lebedev *Zh. Vyschisl. Mat. Mat. Fiz.* **15**,48–54(1975), V.I. Lebedev *Zh. Vyschisl. Mat. Mat. Fiz.* **16**,293–306(1976).

[48]A.J.H. Wachters *J. Chem. Phys* **52**,1033–1036 (1970).

[49]P.J. Hay *J. Chem. Phys* **66**, 4377–4384 (1977).

[50]T. Ziegler and J. Li *Can. J. Chem.*, in press.

[51]F.W. Kutzler and G.S. Painter *Phys. Rev. B*, **43**, 6865 (1991).

[52]D.C. Langreth, and M.J. Mehl *Phys. Rev. B*, **28**, 1809 (1983); **29**, 2310(E) (1984); C.D. Hu and D.C. Langreth *Phys. Scr.*, **32**, 391(1985).

[53]J.P. Perdew and W. Yue *Phys. Rev. B*, **33**, 8800 (1986); J.P. Perdew *Phys. Rev. B*, **33**, 8822 (1986).

[54]R.C. Raffenetti *J. Chem. Phys.* **58**,4452–4458 (1973).

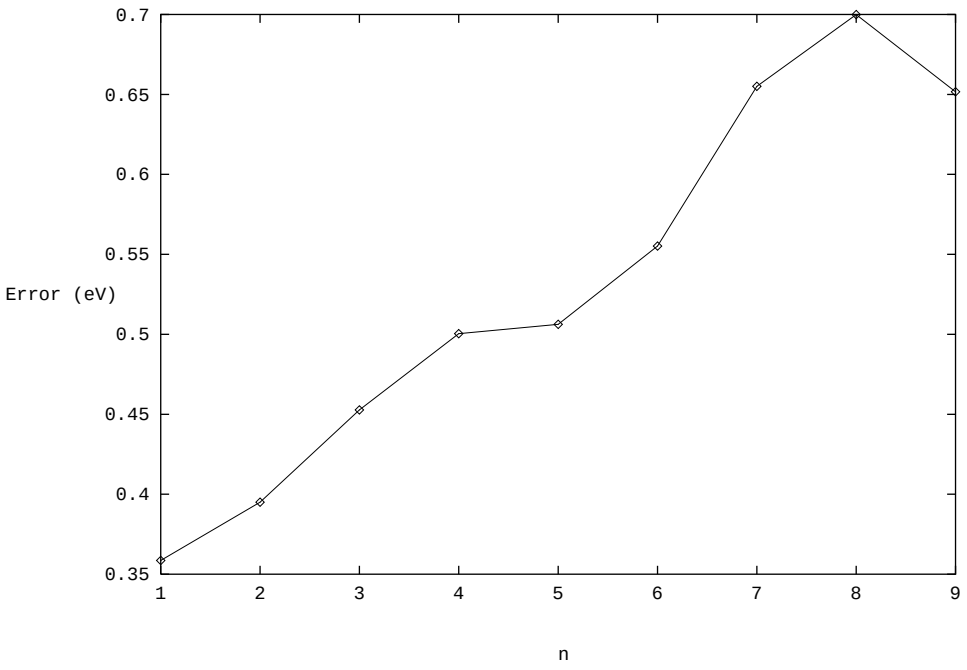
0.7
0.65
0.6
0.55
0.5
0.45
0.4
0.35
Error (eV)
1
2
3
4
5
6
7
8
9
n